

Spin Singlet State in Heptamers Emerging in Spinel Oxide AlV_2O_4

Keisuke MATSUDA*, Nobuo FURUKAWA and Yukitoshi MOTOME¹

Department of Physics and Mathematics, Aoyama Gakuin University, Fuchinobe 5-10-1, Sagamihara, Kanagawa 229-8558

¹ *Department of Applied Physics, University of Tokyo, Hongo 7-3-1, Bunkyo-ku, Tokyo 113-8656*

We present our theoretical results on the electronic state in vanadium spinel oxide AlV_2O_4 . The material is a mixed-valent system with the average valence $\text{V}^{2.5+}$, and V cations constitute a frustrated pyrochlore structure. It shows a structural transition at $\sim 700\text{K}$, leading to the formation of seven V-sites clusters — heptamers. We study the electronic state of the heptamer by explicitly taking account of orbital degree of freedom as well as electron correlations. We show that the ground state of the heptamer for realistic parameters becomes spin-singlet because of strong σ -bonding states of t_{2g} orbitals. Temperature dependence of the magnetic susceptibility in experiments is naturally understood by this singlet formation in heptamers. Our results indicate that in AlV_2O_4 orbital physics is relevant to stabilize a cluster-type singlet state instead of a previously-proposed charge-ordered state with valence skipping.

KEYWORDS: AlV_2O_4 , spinel, pyrochlore lattice, heptamer, spin singlet, exact diagonalization, multi-orbital Hubbard model

1. Introduction

Geometrical frustration in strongly correlated systems has attracted much interests for decades. Many well-studied examples are found in frustrated antiferromagnets, where frustration results in nearly-degenerate ground-state manifolds of a large number of different spin configurations.^{1,2} In some cases, the degeneracy remains down to the lowest temperature and leads to exotic phenomena such as a liquid state and a glassy state. In general, however, nature does not favor the degeneracy, and tries to find a way of lifting it and to select a unique, non-degenerate ground state. It is very intriguing to clarify the mechanism of lifting the degeneracy.

Pyrochlore lattice is a typical frustrated structure in three dimensions, and the magnets on this lattice structure have attracted much attention because of their severe frustration. The pyrochlore lattice consists of a network of corner-sharing tetrahedra, and is regarded as a three-dimensional analogue of Kagomé lattice. In fact, the pyrochlore lattice can be viewed as an alternative stacking of Kagomé and triangular planes as shown in Fig. 1. This lattice structure is found in many real compounds, for instance, in spinels, pyrochlore compounds and cubic Laves-phase intermetallic compounds.

One of the most fundamental problems in the frustrated pyrochlore systems was studied by Anderson.³ He examined the ground state and its degeneracy of the Ising model on the pyrochlore lattice, which mimics a possible charge-ordering phenomenon in magnetite Fe_3O_4 , i.e., the so-called Verwey transition.⁴ He pointed out that the ground state of this model does not exhibit any long-range order and suffers from macroscopic degeneracy. This exemplifies that the frustration may give rise to nontrivial phenomena even in charge degree of freedom. Recently, this ‘charge frustration’ is an issue also in several other mixed-valent materials such as CuIr_2S_4 ⁵ and LiV_2O_4 .^{6,7}

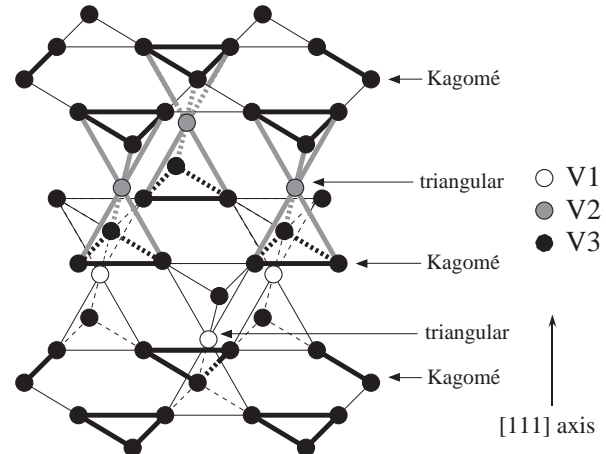


Fig. 1. Schematic picture of the lattice structure of AlV_2O_4 . For simplicity, only V sites are shown, which constitute the pyrochlore structure. There are three crystallographically-inequivalent V sites (V1, V2 and V3), and V-V bond lengths are substantially different below the structural transition temperature $T_c \sim 700\text{K}$. Trimers are shown by bold lines. Two trimers sandwiches a V2 site (connected by gray lines), forming a heptamer. See the text for details.

A spinel oxide AlV_2O_4 is a typical system where this charge-frustration phenomenon is addressed. In this compound, vanadium cations form the pyrochlore lattice and their average valence is $2.5+$. The vanadium cations locate at the octahedral positions, and therefore, five-fold d levels of vanadium are split by the crystal field into low-energy three-fold t_{2g} levels and high-energy two-fold e_g levels. Hence, we have 2.5 d electrons in the three-fold t_{2g} levels on average. Because the t_{2g} levels are partially filled, orbital degree of freedom is also relevant in this compound in addition to charge and spin degrees of freedom. Therefore, AlV_2O_4 is an interesting system to study the effects of geometrical frustration and the roles of charge, spin and orbital degrees of freedom.

AlV_2O_4 shows a phase transition at $T_c \sim 700\text{K}$. At

this temperature, a structural change is observed from high-temperature cubic phase to low-temperature rhombohedral phase accompanied by a doubling of the unit cell along the [111] direction.^{8,9} This transition was interpreted as a charge ordering with valence skipping in which the charge distribution is differentiated between two different [111] planes, namely, Kagomé and triangular planes in Fig. 1; it is supposed that V cations in Kagomé layers take the valence 2+ and those in triangular layers take 4+. However, there remain two puzzles in this charge-ordering scenario. One is the discrepancy between the periodicity of lattice structure and the charge order. The lattice unit cell is doubled in the [111] direction, which is twice longer than that of charge order. The other puzzle is the temperature dependence of the magnetic susceptibility. The susceptibility shows a sudden drop at T_c followed by a Curie-like component in the low-temperature phase. It is difficult to explain this temperature dependence by the charge-ordering scenario.

Recently, the lattice structure of this compound was reinvestigated.¹⁰ It was found that below T_c there is an additional superlattice structure within the Kagomé planes, i.e., a ‘trimer’ formation as shown in Fig. 1. The trimers are paired between neighboring Kagomé planes, which leads to the doubling of the unit cell along the [111] direction. As a result, there are three crystallographically-inequivalent V sites as shown in Fig. 1. Bond lengths between V sites are estimated as 3.04, 2.81, 2.61 and 3.14 Å for V1-V3, V2-V3, short V3-V3 (within trimers) and long V3-V3 (between trimers) bonds, respectively.¹⁰

These substantial difference among the bond lengths imply a decomposition of the whole pyrochlore lattice into two components; one is ‘heptamer’, i.e., a cluster with seven V sites (one V2 site and six V3 sites) connected by bold and gray lines in Fig. 1, and the other is a remaining V1 site. This decomposition and the heptamer formation may provide an alternative scenario to the previous charge-ordering one, which we call the heptamer scenario hereafter. The formation of the heptamer itself naturally explains the doubling of the unit cell along the [111] direction. The peculiar temperature dependence of the susceptibility may also be compromised if one assumes spin-singlet states in the heptamers and local moments at each V1 sites; the former leads to a sudden drop at T_c and the latter gives rise to the Curie-like component below T_c . In fact, it was pointed out that the latter Curie-like component is well fitted by assuming $S = 1$ local moment at each V1 site.¹⁰

From a theoretical point of view, there are two important issues to understand physical properties of AlV_2O_4 on the basis of the heptamer scenario. (i) Why are the heptamers stabilized in this frustrated pyrochlore system? (ii) How does the spin-singlet state emerge in each heptamer? To answer the first question, it is necessary to consider charge, spin and orbital degrees of freedom in the entire pyrochlore lattice, which is very complicated. The second question is also nontrivial. There are totally 18 d electrons in each heptamer when we assign 2 d electrons to each V1 site to form the $S = 1$ moment for the Curie-like contribution. It is not trivial whether we

obtain spin-singlet state with 18 electrons on the seven-sites cluster when we take account of the charge, spin and orbital states as well as electron correlations.

In this paper, we will investigate the second problem, that is, the mechanism of the spin-singlet formation, by studying the electronic state of one heptamer explicitly. We will discuss effects of orbital-dependent transfer integrals, electronic correlations and the crystal field, and clarify the parameter regime where the spin-singlet ground state is obtained. This systematic study provides a simple physical picture of the spin-singlet formation in the heptamer. We believe that the stabilization mechanism of the spin-singlet state may give a hint for the first question as well.

This paper is organized as follows. In §2, we introduce a heptamer Hamiltonian on the basis of multi-orbital Hubbard model. Two different singlet states in the non-interacting case are discussed in §3. In §4, we show our numerical results for the electronic state of the heptamer Hamiltonian. Section 5 is devoted for summary and concluding remarks.

2. Heptamer Hamiltonian

In order to consider the electronic state of one heptamer, we start from a multi-orbital Hubbard model with three-fold t_{2g} orbital degeneracy. The Hamiltonian consists of three terms as

$$\mathcal{H}_{\text{full}} = \mathcal{H}_{\text{kin}} + \mathcal{H}_{\text{int}} + \mathcal{H}_{\text{trig}}, \quad (1)$$

where \mathcal{H}_{kin} describes the kinetic term by electron hoppings between V sites, \mathcal{H}_{int} represents the on-site Coulomb interactions, and $\mathcal{H}_{\text{trig}}$ is for the crystal-field splitting of t_{2g} levels by the trigonal distortion of VO_6 octahedra. The Hamiltonian is defined on the seven-sites cluster in Fig. 2(a), and contains 18 electrons totally as mentioned in §1.

The first term \mathcal{H}_{kin} is given in the form

$$\mathcal{H}_{\text{kin}} = - \sum_{\langle ij \rangle} \sum_{\gamma, \gamma'} \sum_{\tau} t_{ij}^{\gamma\gamma'} (c_{i\gamma\tau}^{\dagger} c_{j\gamma'\tau} + \text{H.c.}), \quad (2)$$

where i, j and $\tau (= \uparrow, \downarrow)$ are site and spin indices, respectively, and $\gamma, \gamma' = 1 (d_{xy}), 2 (d_{yz})$ and $3 (d_{zx})$ are orbital indices. The site indices take the values from 0 to 6 as shown in Fig. 2(a), and the summation $\langle ij \rangle$ is taken over the nearest-neighbor sites. (At this stage, we neglect the difference between the bond lengths of V2-V3 bonds and V3-V3 bonds in the heptamer.) The heptamer originally consists of the edge-sharing network of VO_6 octahedra as shown in Fig. 2(b). For the edge-sharing configuration, the d - d transfer integrals $t_{ij}^{\gamma\gamma'}$ have three different elements for the σ -, π - and δ -bonds depending on the orbital states as shown in Figs. 2(c)-(e).

The Coulomb interaction term \mathcal{H}_{int} consists of the four contributions as

$$\mathcal{H}_{\text{int}} = \mathcal{H}_U + \mathcal{H}_{U'} + \mathcal{H}_J + \mathcal{H}_{J'}, \quad (3)$$

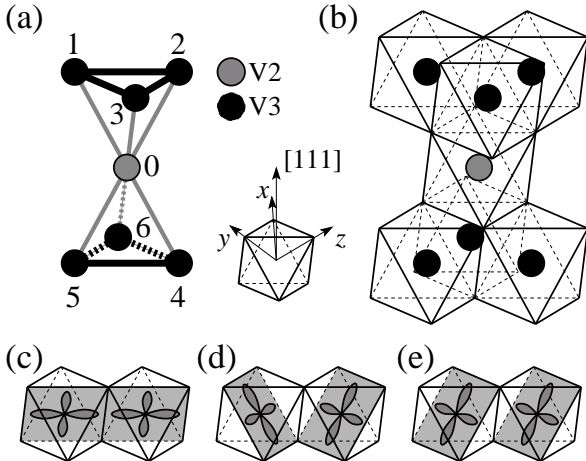


Fig. 2. (a) One heptamer. Site numbering used in our model is shown. (b) Edge-sharing network of VO₆ octahedra for the heptamer. Oxygens are at the corners of octahedra. Transfer integrals between t_{2g} orbitals for (c) σ -, (d) π - and (e) δ -bond, respectively.

where

$$\mathcal{H}_U = U \sum_i \sum_{\gamma} n_{i\gamma\uparrow} n_{i\gamma\downarrow}, \quad (4)$$

$$\mathcal{H}_{U'} = U' \sum_i \sum_{\gamma > \gamma'} n_{i\gamma} n_{i\gamma'}, \quad (5)$$

$$\mathcal{H}_J = J \sum_i \sum_{\gamma > \gamma'} \sum_{\tau, \tau'} c_{i\gamma\tau}^\dagger c_{i\gamma'\tau} c_{i\gamma'\tau'}^\dagger c_{i\gamma\tau'}, \quad (6)$$

$$\mathcal{H}_{J'} = J' \sum_i \sum_{\gamma \neq \gamma'} c_{i\gamma\uparrow}^\dagger c_{i\gamma'\uparrow} c_{i\gamma\downarrow}^\dagger c_{i\gamma'\downarrow}. \quad (7)$$

Here \mathcal{H}_U , $\mathcal{H}_{U'}$, \mathcal{H}_J and $\mathcal{H}_{J'}$ denote the intra- and inter-orbital Coulomb interactions, the exchange interaction and the pair-hopping term, respectively. The density operators are defined by $n_{i\gamma\tau} = c_{i\gamma\tau}^\dagger c_{i\gamma\tau}$ and $n_{i\gamma} = \sum_{\tau} n_{i\gamma\tau}$.

The third term in eq. (1), $\mathcal{H}_{\text{trig}}$, describes the effect of trigonal distortion of VO₆ octahedra. The lattice structure determined by experiments indicates that the VO₆ octahedron including the V2 site is substantially compressed in the [111] direction.¹⁰ The trigonal distortion leads to the crystal-field splitting of three-fold t_{2g} levels at the V2 site into the low-energy a_{1g} singlet and the high-energy e_g doublet. This crystal-field effect is described by

$$\mathcal{H}_{\text{trig}} = -\frac{D}{2} \sum_{\gamma > \gamma'} \sum_{\tau} \left(c_{0\gamma\tau}^\dagger c_{0\gamma'\tau} + \text{H.c.} \right). \quad (8)$$

The compression of VO₆ corresponds to a positive D , and the energy splitting between the a_{1g} singlet and the e_g doublet is $3D/2$ in this definition. We neglect small distortions of octahedra including V3 sites for simplicity.

The multi-orbital Hubbard model (1) is too complicated to fully handle its electronic state, but we can make a simplification on the basis of the lattice structure determined by the experiment. The key observation is that the length of the V3-V3 bonds is considerably shorter than

that of V2-V3 bonds. In fact, the V3-V3 bonds in the heptamer are the shortest ones in the original pyrochlore system, constituting the trimers in the Kagomé layers. Hence, we expect that the σ -bond transfer integrals for these V3-V3 bonds are the most dominant among various contributions in $t_{ij}^{\gamma\gamma'}$. From this observation, we assume that the σ -type bonding state for each V3-V3 bond has low enough energy and fully occupied by two d electrons per bonding state, forming a singlet. For example, the site $i = 1$ is on two V3-V3 bonds ($i, j = (1, 2)$ and $(1, 3)$) which lie in the yz and zx planes, respectively, and therefore, the d_{yz} and d_{zx} orbitals constitute the bonding levels. This is indeed the case in the non-interacting limit $\mathcal{H}_{\text{int}} = 0$, and is supposed to be valid in the weak-correlation regime. The inter-orbital interactions at V3 sites will be taken into account within the Hartree approximation [see eq. (14)].

The assumption of the dominant σ -type V3-V3 bonds allows us to simplify the model defined by eq. (1) in the following points. (i) Since there are six V3-V3 bonds in the heptamer, $6 \times 2 = 12$ electrons occupy the σ -type bonding states. These 12 electrons become inactive on the σ -type V3-V3 bonds. Because we have totally 18 electrons in the model (1), we will consider the remaining 6 electrons in the following calculations. Hereafter, we call the orbitals constituting the σ -type V3-V3 bonds inactive orbitals and the remaining orbitals active orbitals. (ii) All δ -type transfer integrals t_{ij}^{δ} [Fig. 2(e)] can be neglected, because orbitals which are connected to active orbitals through by δ -bonds are always inactive. (iii) π -type transfer integrals for V2-V3 bonds can be also neglected by a similar reason in the above (ii). As a consequence of these simplifications, among the transfer integrals, only two contributions are relevant; one is the σ -bond transfer integral for V2-V3 bonds, which is denoted by $t_{\text{V2-V3}}^{\sigma}$, and the other is the π -bond one for V3-V3 bonds, $t_{\text{V3-V3}}^{\pi}$.

Consequently, on the basis of the above assumption, the Hamiltonian (1) is simplified into the form

$$\mathcal{H} = \tilde{\mathcal{H}}_{\text{kin}} + \tilde{\mathcal{H}}_{\text{int}} + \mathcal{H}_{\text{trig}}. \quad (9)$$

The kinetic term for the remaining 6 electrons, $\tilde{\mathcal{H}}_{\text{kin}}$, reads

$$\tilde{\mathcal{H}}_{\text{kin}} = \mathcal{H}_{\text{kin}}^{\text{V2-V3}} + \mathcal{H}_{\text{kin}}^{\text{V3-V3}}, \quad (10)$$

where $\mathcal{H}_{\text{kin}}^{\text{V2-V3}}$ describes the σ -type hoppings between the V2 site ($i = 0$) and V3 sites ($i = 1 - 6$), and $\mathcal{H}_{\text{kin}}^{\text{V3-V3}}$ denotes the π -type hoppings between the nearest-neighbor V3 sites:

$$\mathcal{H}_{\text{kin}}^{\text{V2-V3}} = -t_{\text{V2-V3}}^{\sigma} \sum_{i=1}^6 \sum_{\tau} \left(c_{0\alpha_i\tau}^\dagger c_{i\alpha_i\tau} + \text{H.c.} \right), \quad (11)$$

$$\mathcal{H}_{\text{kin}}^{\text{V3-V3}} = -t_{\text{V3-V3}}^{\pi} \sum_{\langle ij \rangle \in \text{V3}} \sum_{\tau} \left(c_{i\alpha_i\tau}^\dagger c_{j\alpha_j\tau} + \text{H.c.} \right). \quad (12)$$

Here α_i denotes the active orbital at the i -th V3 sites [for instance, $\alpha_1 = 1$ (d_{xy})]. Note that in eq. (11) the orbital α_i constitutes the σ -bond between 0-th and i -th sites, while the orbitals α_i and α_j at neighboring V3 sites constitute the π -bond in eq. (12) where the summation is

taken over the nearest-neighbor V3 sites. The Coulomb interaction term in eq. (9) is written by

$$\tilde{\mathcal{H}}_{\text{int}} = \mathcal{H}_{\text{int}}^{\text{V2}} + \mathcal{H}_{\text{int}}^{\text{V3}}. \quad (13)$$

The former term is for the V2 site, given by the terms in eq. (3) for $i = 0$ only. The latter is for the V3 sites, which is reduced into

$$\mathcal{H}_{\text{int}}^{\text{V3}} = U \sum_{i=1}^6 n_{i\alpha_i\uparrow} n_{i\alpha_i\downarrow} + (2U' - J) \sum_{i=1}^6 n_{i\alpha_i}, \quad (14)$$

where α_i denotes the active orbital as in eqs. (11) and (12). Here, the second term is the Hartree potential from electrons in the σ -type bonding states assumed for the V3-V3 bonds.

3. Non-interacting Case: Two Different Scenarios for the Singlet Formation

Before going into the numerical study of the electronic state of the heptamer model (9), here we consider the non-interacting case, i.e., $\tilde{\mathcal{H}}_{\text{int}} = 0$ ($U = U' = J = J' = 0$). In this case, we have three parameters $t_{\text{V2-V3}}^{\sigma}$, $t_{\text{V3-V3}}^{\pi}$ and D .

There are two important cases in this parameter space to consider the singlet formation in the heptamer. One is $t_{\text{V2-V3}}^{\sigma} \neq 0$ and $t_{\text{V3-V3}}^{\pi} = D = 0$. The σ -type transfer integrals in an orbital sector (say d_{xy}) have finite matrix elements on one straight V3-V2-V3 bond lying in the corresponding plane (in the xy plane). Hence, in this case, three-sites clusters are formed on straight V3-V2-V3 bonds in each orbital sector, for instance, a cluster with the sites $i = 1, 0, 4$ in the d_{xy} orbital sector. In each cluster, the ground state is given by the bonding state of three sites, being singlet as shown in Fig. 3(a). The ground-state wave function for the heptamer is given by

$$|\sigma\rangle = \prod_{\tau} \prod_{i=1}^3 \frac{1}{2} \left(c_{i\alpha_i\tau}^{\dagger} + \sqrt{2} c_{0\alpha_i\tau}^{\dagger} + c_{(i+3)\alpha_i\tau}^{\dagger} \right) |0\rangle, \quad (15)$$

where $|0\rangle$ is the vacuum state of the model (9). We call this the σ -type singlet. Note that the state (15) is obtained for both positive and negative $t_{\text{V2-V3}}^{\sigma}$.

The other important case is $t_{\text{V2-V3}}^{\sigma} = 0$ and $t_{\text{V3-V3}}^{\pi}, D > 0$. In this case, the heptamer is disconnected into the isolated V2 site and two trimers with V3 sites. In each trimer, the ground state is given by the bonding state due to the π -type transfer integrals, $t_{\text{V3-V3}}^{\pi}$. At the V2 site, for a positive D , the ground state is given by doubly-occupied a_{1g} singlet as shown in Fig. 3(b). Hence the wave function for the heptamer reads

$$|\pi\rangle = \prod_{\tau} \sum_{\gamma=1}^3 \frac{c_{0\gamma\tau}^{\dagger}}{\sqrt{3}} \sum_{i=1}^3 \frac{c_{i\alpha_i\tau}^{\dagger}}{\sqrt{3}} \sum_{i=4}^6 \frac{c_{i\alpha_i\tau}^{\dagger}}{\sqrt{3}} |0\rangle. \quad (16)$$

This state is schematically shown in Fig. 3(b). We call this the π -type singlet. Note that if $t_{\text{V3-V3}}^{\pi}$ or D is negative, the ground state becomes no longer singlet and has some degeneracy.

When we switch on the interactions, it is non-trivial that the ground state is singlet. Nevertheless, as we will see in numerical results in the next section, there appear two different singlet regimes; one includes the σ -singlet

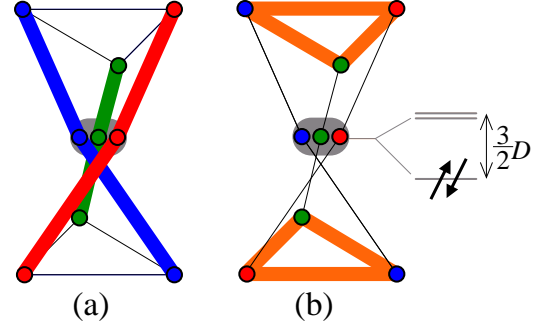


Fig. 3. Schematic pictures of two different singlet states in the non-interacting case, (a) σ -singlet state [eq. (15)] and (b) π -singlet state [eq. (16)]. Blue, red and green circles represents d_{xy} , d_{yz} and d_{zx} orbitals at each V site, respectively. Singlet bonds are shown by bold lines. In (b), at V2 site, two electrons occupy the a_{1g} singlet state due to the trigonal splitting.

case and the other includes the π -singlet one. In other words, in each regime, the wave function is adiabatically connected with either of $|\sigma\rangle$ or $|\pi\rangle$. Thus, our questions are twofold. (i) For realistic values of parameters, does the ground state of the heptamer Hamiltonian become singlet? (ii) If that is the case, which category does the singlet state belong to, the σ - or π -singlet state?

4. Effects of Electron Correlation: Exact Diagonalization Study

4.1 Method and parameters

We investigate the electronic state of the model (9) including the interaction terms by exact diagonalization (ED). We use Householder method for the ED calculations.

For the d - d transfer integrals, the Slater-Koster scheme¹¹ gives the estimates $t_{\text{V2-V3}}^{\sigma} \simeq 0.5\text{eV}$ and $t_{\text{V3-V3}}^{\pi} \simeq -0.26\text{eV}$ by using the bond lengths in experiments. Hereafter we set $t_{\text{V2-V3}}^{\sigma} = 1$ as an energy unit, and change $t_{\text{V3-V3}}^{\pi}$ from -2 to 2 and D from 0 to 2 to study overall features in the parameter space.

Concerning the interaction parameters, experimental estimate for AlV_2O_4 is not available yet. An estimate was given for a related spinel vanadate LiV_2O_4 ;¹² the optical measurement suggests $U \gtrsim 2\text{eV}$. In the following, we present the results for $U = 0 - 8$ to show the tendency with changing U . We set $J = 0.1U$, and retain the relations $U = U' + 2J$ and $J = J'$.¹³

4.2 Results

First, we study the degeneracy of the ground state of the heptamer Hamiltonian (9). Figure 4 shows the degeneracy in the $t_{\text{V3-V3}}^{\pi}$ - D plane for different values of U . Singlet ground states without any degeneracy are obtained in two separated regions in the present parameter space. Each region includes one of the limits in the non-interacting case discussed in §3; one region extends from the σ -singlet limit ($t_{\text{V3-V3}}^{\pi} = D = U = 0$), and the other region at $t_{\text{V3-V3}}^{\pi}, D \gg t_{\text{V2-V3}}^{\sigma}$ and $U = 0$ continues to the π -singlet limit ($t_{\text{V2-V3}}^{\sigma} = U = 0$ and $t_{\text{V3-V3}}^{\pi}, D > 0$). Both singlet regimes shrink as U increases, but remain well for intermediate or rather large values of U .

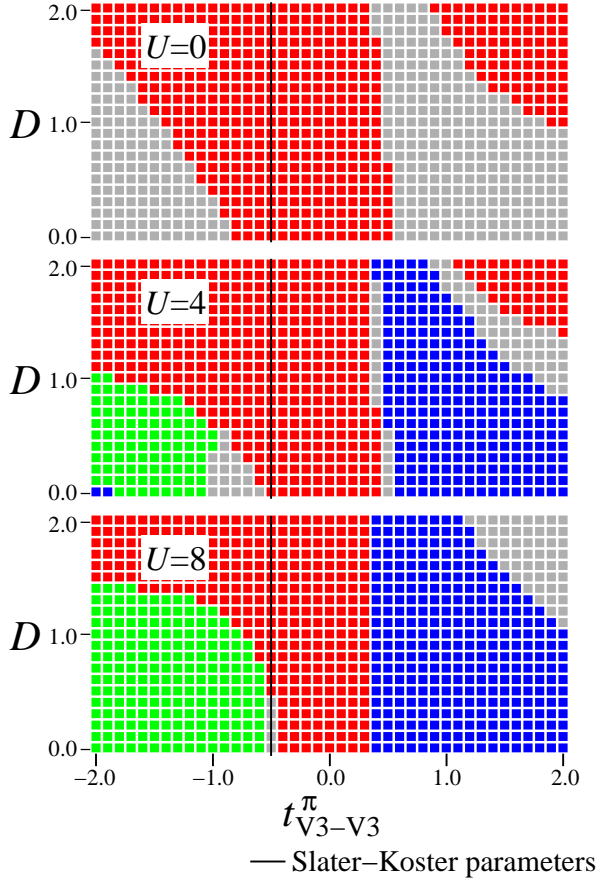


Fig. 4. Degeneracy of the ground state of the heptamer model for several U .

Although these two singlet regions are separated in the parameter space, the ground states for two regions show the same symmetry. The symmetry of the ground state of the model (9) belongs to one of the irreducible representations A_1 , A_2 and E because the Hamiltonian belongs to D_3 point group.¹⁵ We calculate $\langle \phi_0 | C_3 | \phi_0 \rangle$ and $\langle \phi_0 | C'_2 | \phi_0 \rangle$, where C_3 and C'_2 are symmetric rotation operator of three-fold symmetric axis by $3\pi/2$ of two-fold symmetric axis by π , respectively. Here, $|\phi_0\rangle$ is the ground-state wave vector obtained by ED calculations. We found that $\langle \phi_0 | C_3 | \phi_0 \rangle = \langle \phi_0 | C'_2 | \phi_0 \rangle = 1$ for all the ED solutions without degeneracy. Namely, all the ground states in both separated singlet regions belong to A_1 symmetry group.

To characterize two singlet regimes, we calculate overlaps of the ground-state wave function with $|\sigma\rangle$ and $|\pi\rangle$ in eqs. (15) and (16), respectively. Figure 5 plots the difference of the absolute values of two overlaps;

$$\Psi = |\langle \sigma | \phi_0 \rangle| - |\langle \pi | \phi_0 \rangle|. \quad (17)$$

As $\langle \sigma | \pi \rangle = 0$, this quantity measures how the ED solution is close to two singlet states in the non-interacting case. As shown in Fig. 5, two different singlet regions show distinct behavior. In one region including the σ -singlet limit, Ψ is almost 1, that is, the ground state is close to $|\sigma\rangle$. In the other region including the π -singlet limit, Ψ becomes almost -1 , that is, the ground state looks like $|\pi\rangle$. Two regimes are well separated and Ψ are

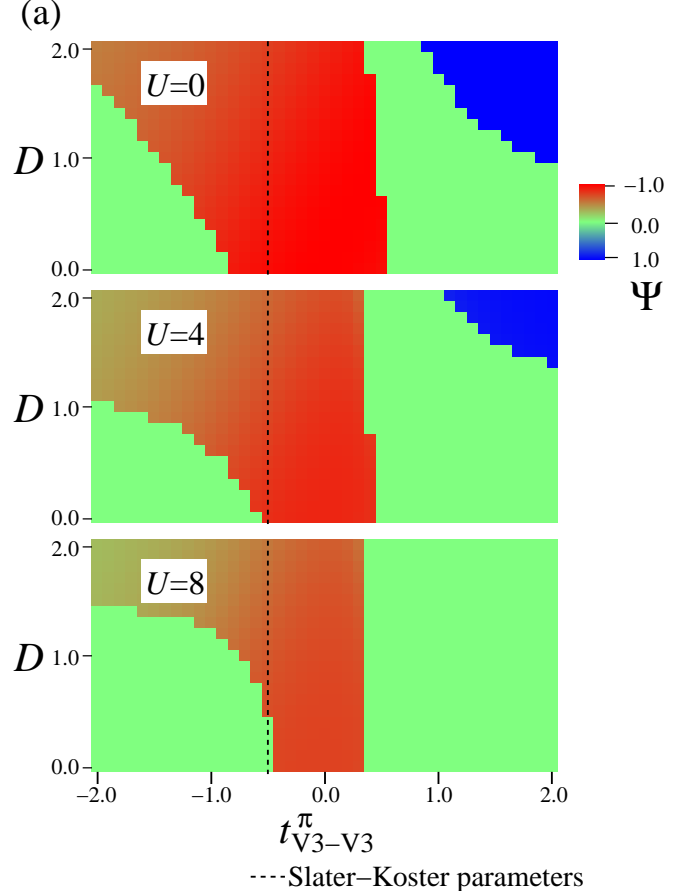


Fig. 5. (a) The overlap parameter Ψ [eq. (17)] for several U . U dependences are shown in (b) for several sets of (t_{V3-V3}^π, D) . The solid lines in (b) are guides for the eyes. In the degenerate regions, we plot the values averaged over all degenerate states.

discontinuous between the non-degenerated and degenerated regions for all values of U .

We also calculate the charge disproportionation between the V2 site and the V3 sites. Figure 6 shows the electron density at the V2 site;

$$N_2 = \langle \phi_0 | \sum_{\gamma} n_{0\gamma} | \phi_0 \rangle. \quad (18)$$

Note that the electron density at the V3 site is given by $(18 - N_2)/6$ for singlet states with A_1 symmetry. In the σ -singlet region, as U increases, N_2 continuously decreases from the non-interacting value 3. On the con-

trary, in the π -singlet region, N_2 is almost unchanged and remains at the non-interacting value 2. This difference comes from the nature of the singlet states. In the former, since the dominant singlet bonds are on the straight V3-V2-V3 clusters, electron charges are easily redistributed between V2 and V3 sites. On the other hand, in the latter π -singlet regime, the dominant singlet bonds are confined within V3 trimers, and the bonds between V2 and V3 sites are rather weak. There, the singlet energy gain within the V3 trimers as well as the crystal field D at the V2 site prevents the charge redistribution between V2 and V3 sites.

The results in Figs. 4 and 5 show that for the estimates of transfer integrals by using the Slater-Koster scheme, the ground state of the model (9) is singlet and belongs to the σ -singlet regime where the ground-state wave function is close to $|\sigma\rangle$ in eq. (15). We note that the π -singlet like state is only limited to a region where t_{V2-V3}^π and D are both larger than t_{V2-V3}^σ , and this is not realistic in the present t_{2g} electron system. Therefore, we conclude that the singlet ground state is realized in the heptamer, and that the basic mechanism of the singlet formation is understood by the σ -bonding of t_{2g} orbitals.

Finally, we calculate the energy gap from the singlet ground state to the first excited state for a comparison with experimental data. The result is shown in Fig. 7 for the Slater-Koster parameters. In fact, the gap in Fig. 7 gives the spin gap from the singlet ground state. To show this, we calculate

$$S_1^z = \sum_{k=1}^{m_1} |\langle \phi_{1,k} | S^z | \phi_{1,k} \rangle|, \quad (19)$$

where m_1 is the degeneracy of the first excited state, $|\phi_{1,k}\rangle$ is the k -th state in the manifold of the first excitation, and S^z is the z component of the total spin. We found that $S_1^z \neq 0$ for all the ED solutions in the region where the ground state is non-degenerate. This indicates that the first excited states are magnetic and we can regard the energy gap in Fig. 7 as the spin gap. The experimental estimate of the spin gap is given by the fit of temperature dependence of the magnetic susceptibility,¹⁰ and shown in Fig. 7 as the horizontal dashed line. We note that our results in Fig. 7 approach the experimental estimate, particularly for intermediate or large U , but are still larger. This is not surprising because here we do not take into account interactions among heptamers which will reduce the gap. Thus, our results on the gapped, spin-singlet ground state in the heptamer model support the heptamer picture, in which the peculiar temperature dependence of the magnetic susceptibility is explained as the summation of the heptamer-singlet contribution and the $S = 1$ Curie-like contribution.¹⁰

5. Summary and Concluding Remarks

We have investigated the origin of spin-singlet formation in seven-sites clusters, heptamers, which emerge in the spinel oxide AlV_2O_4 as a result of the structural change with the trimer formation in Kagomé layers of V pyrochlore lattice. We have derived an effective model to describe the charge, spin and orbital degrees of freedom in one heptamer from the Hubbard model with t_{2g}

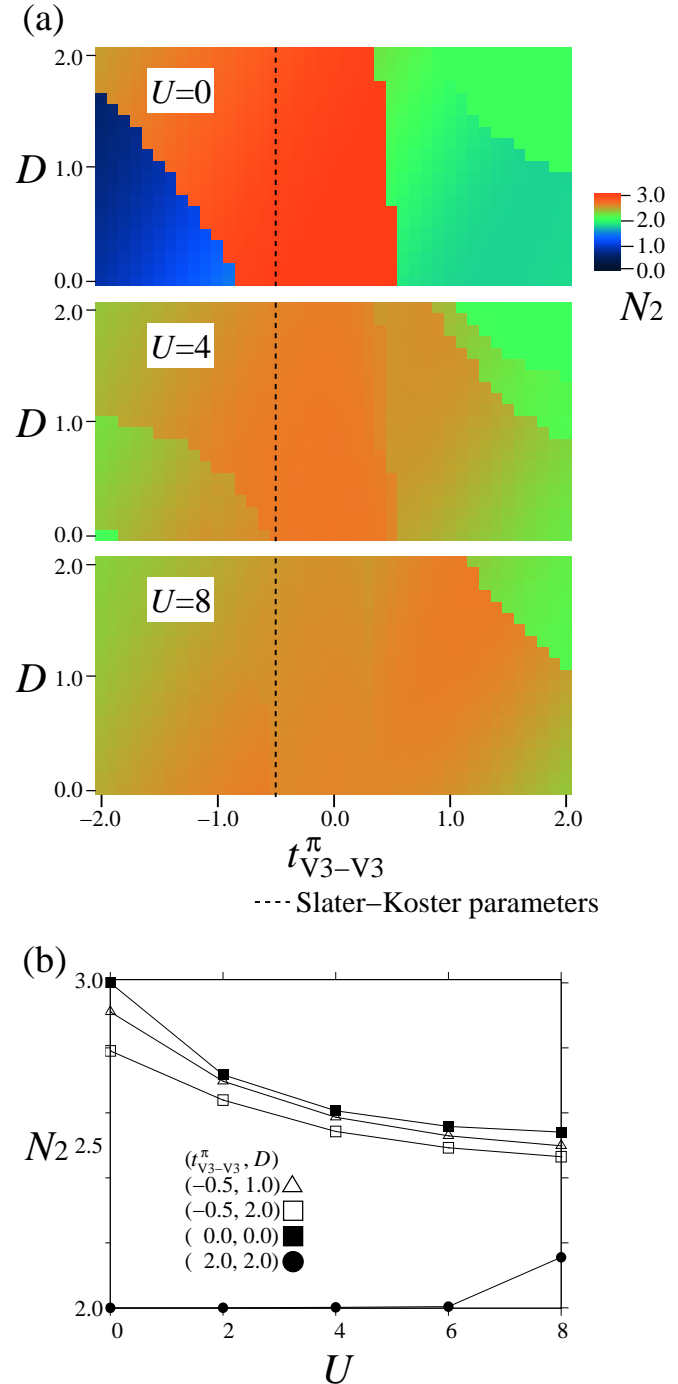


Fig. 6. (a) Charge density at V2 site, N_2 for several U . U dependences are shown in (b) for several sets of (t_{V3-V3}^π, D) . The solid lines in (b) are guides for the eyes. In the degenerate regions, we plot the values averaged over all degenerate states.

orbital degeneracy, and investigated its electronic and magnetic states by using numerical exact diagonalization. Our results indicate that in realistic parameter region for AlV_2O_4 , the ground state of the heptamer becomes spin-singlet, and that not the trimer formation in the Kagomé layers but the heptamer formation plays an essential role on the spin-singlet formation in this system. We conclude that the singlet state is stabilized by dominant $d-d$ transfer integrals of σ -type which form bonding states within the heptamer. The heptamer formation can give a comprehensive understanding of the magnetic

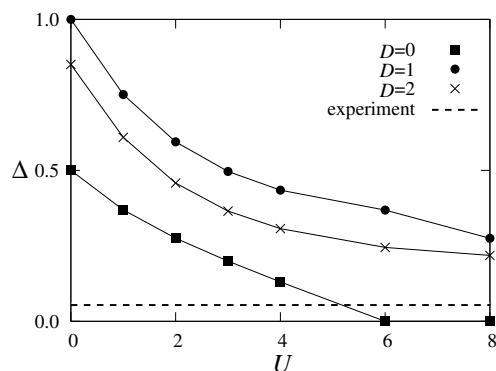


Fig. 7. Spin gap for the heptamer model (9) for $t_{V3-V3}^\pi = -0.5$. The dashed line represents the spin gap estimated experimentally.¹⁰

properties observed in experiments; a suppression due to the singlet gap formation and the Curie-like behavior at lower temperatures coming from $S = 1$ moments outside the heptamers.

How to distinguish experimentally two different origins of the singlet formation, σ - or π -type? One possible way is to detect the directional dependence of the spin excitation. The dominant singlet bonds lie on the intertrimer V3-V2-V3 bonds in the σ case and within the V3 trimers on Kagomé planes in the π case. This difference may be detected by using Raman scattering technique. Another possibility is to measure the local density of d electrons at V2 site. Our results in Fig. 6 (f) indicate that the local density becomes $\sim 2.5 - 3.0$ for the σ -type singlet state, while it is $\simeq 2.0$ for the π -type one.

Let us comment on properties of $S = 1$ moments outside the heptamers. In AlV_2O_4 , at much lower temperature than T_c , another anomaly appears at $T \sim 5\text{K}$, which is ascribed to spin-glass transition.⁸ In our heptamer scenario, magnetic moments remaining active below T_c are the $S = 1$ spins at V1 sites. These moments are rather far apart from each other: The nearest-neighbor V1 pairs correspond to the third-neighbor sites across hexagons in the original pyrochlore lattice, forming two-dimensional triangular lattice in the [111] planes. Hence, the $S = 1$ moments at V1 sites constitute a weakly-coupled triangular spin system at low temperatures. The sign of exchange interactions is not trivial because of complicated exchange paths, but in any case, it is believed that Heisenberg spin systems on weakly-coupled triangular lattice show a magnetic order, not a spin-glass behavior. Therefore, our heptamer scenario suggests that the spin-glass behavior comes from an extrinsic effect, such as randomness.

Our present study is on the basis of the lattice structure below the structural transition temperature, and therefore, at this stage cannot answer why and how the lattice distortion including the formation of heptamers is stabilized in the frustrated pyrochlore lattice structure. There are many similar examples of such clusters in frustrated systems, such as hexamer in ZnCr_2O_4 ,¹⁶

octamer in CuIr_2S_4 ,^{5,17} trimer in LiVO_2 ,¹⁸ and dodecamer in double-exchange spin-ice model on a Kagomé lattice.¹⁹ These facts suggest a ubiquitous role of cluster formations to lift the degeneracy inherent in frustrated systems although the driving force may depend on the details of systems. In the present system AlV_2O_4 , our results imply that the stability of the heptamer singlet state itself may play some role on the mechanism of self-organizing the clusters. However, in order to identify a dominant player, it is necessary to handle charge, spin, orbital and lattice degrees of freedom and to compare the instabilities to many possible ordered states on the frustrated pyrochlore lattice. This is left for future study.

Acknowledgment

We would like to thank M. Shingu, T. Katsufuji, S. Mori and Y. Horibe for stimulating discussions. This work was supported by a Grant-in-Aid for 21st COE program and for Scientific Research (No. 16GS50219) from the Ministry of Education, Culture, Sports, Science and Technology of Japan.

- 1) *Magnetic System with Competing Interaction*, ed. by H. T. Diep (World Scientific Publishing Co., 1994).
- 2) R. Liebmann, *Statistical mechanics of periodic frustrated Ising systems* (Springer-Verlag, Berlin, Tokyo, 1986).
- 3) P. W. Anderson: Phys. Rev. **102** (1956) 1008.
- 4) E. J. W. Verwey: Nature (London) **144** (1939) 327.
- 5) P. G. Radaelli, Y. Horibe, M. J. Gutmann, H. Ishibashi, C. H. Chen, R. M. Ibberson, Y. Koyama, Y. S. Hor, V. Kiryukhin, S-W. Cheong: Nature **416** (2002) 155.
- 6) S. Kondo, D. C. Johnston, C. A. Swenson, F. Borsa, A. V. Mahajan, L. L. Miller, T. Gu, A. I. Goldman, M. B. Maple, D. A. Gajewski, E. J. Freeman, N. R. Dilly, R. P. Dickey, J. Merrin, K. Kojima, G. M. Luke, Y. J. Uemura, O. Chmaissem, and J. D. Jorgensen: Phys. Rev. Lett. **78** (1997) 3729.
- 7) C. Urano, M. Nohara, S. Kondo, F. Sakai, H. Takagi, T. Shiraki, and T. Okubo: Phys. Rev. Lett. **85** (2000) 1052.
- 8) K. Matsuno, T. Katsufuji, S. Mori, Y. Moritomo, A. Machida, E. Nishibori, M. Takata, M. Sakata, N. Yamamoto, and H. Takagi: J. Phys. Soc. Jpn. **70** (2001) 1456.
- 9) K. Matsuno, T. Katsufuji, S. Mori, M. Nohara, A. Machida, Y. Moritomo, K. Kato, E. Nishibori, M. Takata, M. Sakata, K. Kitazawa, and H. Takagi: Phys. Rev. Lett. **90** (2003) 096404.
- 10) Y. Horibe, M. Shingu, K. Kurushima, H. Ishibashi, N. Ikeda, K. Kato, Y. Motome, N. Furukawa, S. Mori, and T. Katsufuji: Phys. Rev. Lett. **96** (2006) 086406.
- 11) J.C. Slater, G.F. Koster: Phys. Rev. **94** (1954) 1498.
- 12) A. Fujimori, K. Kawakami and N. Tsuda: Phys. Rev. B **38** (1988) 7889.
- 13) J. Kanamori: Prog. Theor. Phys. **30** (1963) 275.
- 14) J. Matsuno, A. Fujimori, and L. F. Mattheiss: Phys. Rev. B **60** (1999) 1607.
- 15) Formally, the point group of the Hamiltonian is $D_{3d} = D_3 \otimes C_i$.
- 16) S.-H. Lee, C. Broholm, W. Ratcliff, G. Gasparovic, T. H. Kim, Q. Huang, and S-W. Cheong: Nature **418** (2002) 856.
- 17) D. I. Khomskii and T. Mizokawa: Phys. Rev. Lett. **94** (2005) 156402.
- 18) H. F. Pen, J. van den Brink, D. I. Khomskii, and G. A. Sawatzky, Phys. Rev. Lett. **78** (1997) 1323.
- 19) Y. Shimomura, S. Miyahara and N. Furukawa, J. Phys. Soc. Jpn. **73** (2004) 1623.